TESTING AIR-BREATHING ROCKET ENGINES

MARRIOTT PARK HOTEL, ROME, ITALY / 2 – 6 MAY 2016

Iain Waugh[1], Andrew Davies[1], Ed Moore[1], Helen Webber[2], and James Macfarlane[1],[3]

[1] *Airborne Engineering Ltd., Westcott Venture Park, Aylesbury, HP18 0XB, UK*
[2] *Reaction Engines Ltd., Culham Science Centre, Abingdon, OX14 3DB, UK*
[3] *Corresponding author: james@ael.co.uk*

KEYWORDS:

Air-breathing, altitude compensation, rocket engine, sea-level testing, metering valves

ABSTRACT:

The unique propulsion requirements for air-breathing space planes have resulted in a R&D programme to investigate various aspects of the Sabre engine technology. These include altitude compensation and the requirement to transition from air-breathing mode to pure rocket mode. This paper describes the challenges involved in the design, construction and operation of a test rig for investigating Sabre nozzle and combustor design using a 20KN sub-scale engine. Such challenges include precision control and measurement of mass-flow in non-ideal gases, multi-axis thrust measurement, nozzle wall-pressure profiling and automated analysis of large data sets.

1. INTRODUCTION

Reaching orbit currently requires multiple-stage launchers with expendable stages. Most of the cost of these launches is incurred in producing the launcher itself, rather than the per-launch fuel and logistics costs. A reusable launcher could therefore dramatically reduce the cost of reaching orbit. Furthermore, reducing the number of launcher stages could reduce costs further by decreasing system complexity.

The major problem with achieving orbit with a single or dual stage vehicle is achieving the mass fraction required to reach orbital velocity. This comes directly from the Tsiolovsky rocket equation, where the limiting mass fraction of the vehicle is fixed by the desired change in velocity, and the specific impulse of the exhaust propellants. Even with a high energy propellant combination, such as hydrogen and oxygen, the required mass fraction for single or dual stage vehicles is extremely unforgiving.

The Synergetic Air-Breathing Rocket Engine (SABRE), designed by Alan Bond, Reaction Engines Ltd., aims to mitigate this major problem. The mass fraction requirement of a single or dual stage vehicle is relaxed significantly by using Sabre engines. Sabre engines breathe air for the initial part of the trajectory up to Mach 5.5, which reduces the amount of oxidiser the vehicle needs to carry, and in turn significantly improves the specific impulse of the exhaust propellants in air-breathing mode. For a single stage vehicle, this increases the maximum structural mass fraction requirement for the vehicle from 0.13 to 0.21, which is significant in terms of the feasibility of the vehicle design and the payload weight [1].

To maintain the high engine installed specific impulse and the vehicle structural mass fraction, the design of the combustion chamber and nozzle system is crucial. ‘Dual mode’ nozzles use the same nozzle hardware to expand the exhaust propellants from both air-breathing and rocket modes. This is desirable because of the reduced weight and the potential for reduced nacelle base drag, and therefore has been the basis of a variety of nozzle concepts being explored by Reaction Engines.

Dual mode nozzles have to achieve high specific impulse in two cases: first, in rocket mode, where a high area ratio expansion is required, and second, in air-breathing mode, where the maximum thrust is obtained when the gases are expanded to the ambient pressure and the nozzle flow is full. When the exit pressure is mismatched to the ambient pressure, however, the flow will either be underexpanded, over-

Figure 1: Stern 5kN rocket engine with an expansion-deflection nozzle

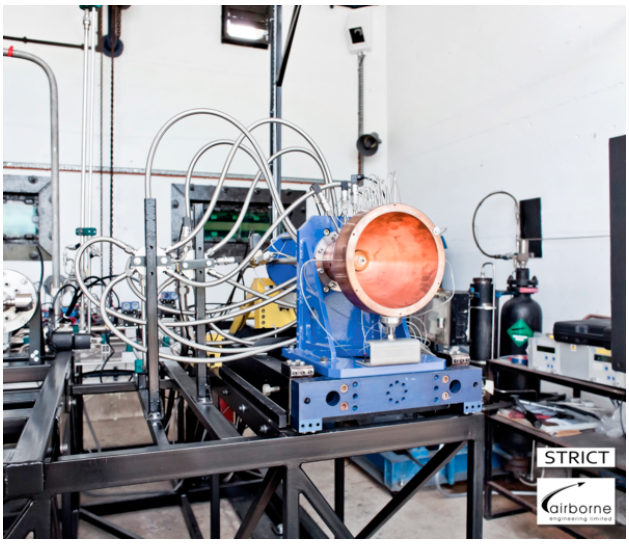

Figure 2: Strict rocket engine with an expansion-deflection nozzle

expanded or separated, with a loss of thrust in each case. A range of altitude compensating nozzles have therefore been considered.

One Sabre concept uses an expansion-deflection (ED) nozzle [2]. An ED nozzle passively increases the area ratio of the flow as the back pressure on the nozzle is dropped, until the nozzle is eventually running full. It has a central pintle to initially direct flow towards the wall of the nozzle once it has passed the throat. The flow then expands around the pintle, enlarging the flow area until it is close to matching the ambient back pressure. A recirculating wake is formed at the rear of the pintle, which may be open at high back pressure, and closed at low back pressure.

With the range of air pressures that variants of the SABRE engine are capable of delivering, Reaction Engines have also been investigating nozzle designs whereby the nozzle system would have to interface with separate air breathing and rocket engine combustion chambers, where the difference in their operational pressures is too great for a single throttlable system. The Stoic engine is one such example, to which this paper specifically refers. The performance, and steady/unsteady aerodynamic behaviour of these annular flow nozzles must be fully characterised before feasibility of their use can be justified.

1.1. Past work: Stern, Strict and Strident engines

ED nozzle concepts have been tested previously for the Sabre engine, most notably at the University of Bristol EMEGG facility [3, 4] and the Stern and Strict engines at the Airborne Engineering Ltd. (AEL) facilities [5]. It has been shown that great care is required to prevent separation of the flow from the nozzle outer wall, but this can be achieved by optimising the geometry of the pintle and nozzle using the axisymmetric method of characteristics [3]. The nozzle efficiency of an optimised ED nozzle can then potentially outperform a a dual-bell nozzle, particularly at high pressure ratios [4].

The Static Test Expansion-deflection Rocket Nozzle (Stern) engine was a 5kN gaseous H_2-Air rocket engine with an ED nozzle and a copper heat-sink chamber. Fig. 1 shows the chamber configuration, which was tested in both cold and hot flow conditions. On the positive side, it demonstrated excellent flow stability on the nozzle walls with no flow separation at any operating condition. On the negative side, however, it showed lower than desired wake pressures leading to higher base drag [5].

The Strict engine was designed as the natural progression from the Stern engine, to encompass the lessons learned during the Stern programme. The Strict engine was tested on gaseous H_2-Air propellants at AEL's Westcott facility in 2011.

Developments in the thermodynamic cycle of the SABRE engine have led to an important change from its original design; specifically the ability to halve the fuel consumption in air-breathing mode by allowing the airflow to combust in a separate low pres-

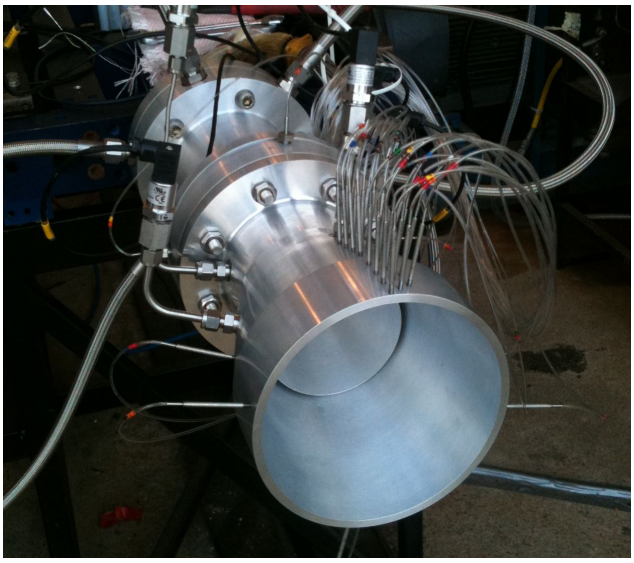

Figure 3: Strident cold flow rocket engine with dual-throat nozzle, as a subscale test article for one of the Sabre engine concepts. The inner 'rocket mode' chamber has a high expansion ratio for near vacuum conditions, and the annular 'air-breathing' mode chamber uses the inner nozzle as the pintle for an ED altitude compensating nozzle.

sure combustion chambers. In order to facilitate the different pressure deliveries of the air-breathing and rocket modes however, whilst maintaining an overall lightweight system with minimal base drag, the airflow is combusted in separate annular chambers which encircle the internal rocket engine combustion chambers[2]. In doing so, the rocket nozzle can be reused for the air-breathing expansion by incorporating a split in the nozzle extension at an appropriate downstream location. In air-breathing mode the extension is withdrawn to allow expansion of the air-breathing combustion products as an annular jet. In rocket mode the extension is translated to allow the rocket exhaust to expand over the full nozzle area ratio for maximum performance. The concept of having a dual throat nozzle was tested using the Strident engine (Fig. 3), which had a realistic geometry but was designed for cold flow testing only.

1.2. Current work: Stoic engine

The Stoic engine is the natural successor from the Strident engine, with full combustion in both combustion chambers. The test rig design for the Stoic engine is the focus of this paper.

The test rig design required particular care in two areas: first, in the measurement and control of the high mass flow gaseous propellant feeds, and second, in the acquisition and dissemination of the large data sets from each test. These areas of the test rig design are discussed in detail, and some engine results are presented to demonstrate the test rig in action.

2. STOIC ENGINE

The Stoic engine was designed as part of the Advanced Nozzle programme (AN) by Reaction Engines Ltd. under ESA funding. The Stoic engine has many subscale features of the Sabre engine, most importantly that it has both air-breathing and rocket modes, and the ability to change between these two modes via a translating nozzle extension. The Stoic engine also encompasses many other novel features such as a 3D printed injector manifold.

There are four major outputs from the AN programme. First, to validate the performance of the dual throat nozzle against CFD simulations. Second, to characterise the off-axis thrust components of the dual throat nozzle, both transiently and in steady state. Third, to test the method of switching between the air-breathing and rocket modes. Fourth, to validate the heat transfer model of the combustion chamber and nozzle, and to test the effect of air-film cooling.

The Stoic engine requires four gaseous propellant streams and six coolant streams. The four propellants consist of air and H_2 for the air-breathing mode, and O_2 and H_2 for the rocket mode. The six coolant streams consist of four water streams for the combustion chamber, nozzle, injector face and other internals, and two air streams for film cooling. Water is used as a coolant to simplify the test engine development; regenerative fuel coolant is used in the Sabre engine.

With the exception of the water coolant, each of these streams affects the mass flow passing through the engine and therefore the thrust and performance of the nozzle. The mass flow of each stream must therefore be known to a high degree of accuracy, specified as $\pm 1\%$. Additionally, the process of switching between the air-breathing and rocket modes requires that these streams are controllable in real-time using feedback from sensor measurements.

The Stoic engine has a thrust rating of 20kN, which requires requires propellant feeds of 0.3kg/s H_2 and 10kg/s of air in air-breathing mode, and 0.5kg/s H_2 and 3.3kg/s O_2 in rocket mode. It requires a total water coolant flow of 20kg/s. The maximum test duration of the cooled engine is 8 seconds.

3. TEST RIG DESIGN

3.1. Propellant supply

The Stoic engine requires high mass flow rates of gaseous propellants at a relatively high delivery pressure to the engine (30-60bar). The propellant gases are supplied from several high pressure reservoirs. The air reservoir consists of a custom manifold of twelve 89 litre gas bottles, which are manifolded together using large bore fittings to maximise the flow rate. The H_2 and O_2 reservoirs are provided by manifolding together pallets of gas bottles as provided by the gas supplier. Unfortunately, most gas providers use very narrow bore fittings at the outlet of each individual bottle, therefore 6 or 7 pallets each are needed to obtain the gas flow rates required without choking or unacceptable pressure loss.

3.2. Automatic metering valves

A custom automatic metering valve (AMV) is installed in the propellant line for each of the gaseous propellants (H_2, O_2 and air) and each of the air film coolant streams. An AMV is necessary because a set mass flow rate is required into the Stoic engine, which must be provided from a reservoir whose pressure drops rapidly during a test. The AMVs allow the Stoic engine to be operated in two modes. First, a fixed mode, where mass flow profiles for each propellant are pre-defined and run from a common clock. Second, a real-time control mode, where mass flows can be controlled based on feedback from measurements of engine parameters. This latter mode is important for controlling the transition between the air-breathing and rocket modes of the Stoic engine.

Each AMV consists of three parts: a venturi meter, a metering valve and a control system. These will be described further in the next few subsections.

3.2.1. Venturi meter

A Venturi meter was chosen for the mass flow measurement section of the AMVs, because they have low pressure loss (<5%), high accuracy and do not require the use of empirically defined coefficients. Other measurement methods, such as orifice meters, require empirical coefficients which are usually defined for hydraulic or for low flow speeds between specific diameter ranges.

The expansion in the Venturi tube is assumed to be isentropic, because there is relatively low pressure loss and relatively low thermal convection to the walls. The mass flow is calculated from the known upstream and throat areas (A_1, A_2) and the three measurements: the pressure and temperature upstream (p_1, T_1), and the pressure at the throat (p_2). Wall effects are ignored and all measurements are assumed to be static rather than stagnation quantities.

The full method for mass flow calculation is:

1. The known values are p_1, T_1, p_2, A_1 and A_2.
2. Calculate the upstream density $\rho_1 = f(p_1, T_1)$, and entropy $s = f(p_1, T_1)$, using the equation of state.
3. Calculate the density at the throat, $\rho_2 = f(p_2, s)$ using the equation of state and iteration.
4. Calculate the upstream and throat enthalpies, $h_1 = f(p_1, T_1)$ and $h_2 = f(p_2, s)$, using the equation of state and iteration.
5. Calculate the upstream velocity by rearranging the adiabatic steady flow energy equation to give: $u_1 = \sqrt{\frac{2(h_1 - h_2)}{\left(\frac{\rho_1 A_1}{\rho_2 A_2}\right)^2 - 1}}$.
6. Calculate mass flow using $\dot{m} = \rho_1 A_1 u_1$.

A simplified method assumes that γ is constant over the local range of pressures and temperatures in the expansion. A closed form expression can be defined based on the five knowns and two other values: the upstream density $\rho_1 = f(p_1, T_1)$ and the ratio of specific heats $\gamma = f(p_1, T_1)$.

$$\dot{m} = \frac{C_d A_2 \sqrt{\frac{2 p_1 \rho_1 \gamma}{\gamma - 1}\left[\left(\frac{p_2}{p_1}\right)^{\frac{2}{\gamma}} - \left(\frac{p_2}{p_1}\right)^{1+\frac{1}{\gamma}}\right]}}{\sqrt{1 - \left(\frac{A_2}{A_1}\right)^2 \left(\frac{p_2}{p_1}\right)^{\frac{2}{\gamma}}}} \quad (1)$$

For both these methods an equation of state is required to calculate the required flow properties. A real gas model must be used because the reservoir pressures (150-200bar) are high enough that compressibility effects become significant. For example, the density of hydrogen at 200bar and 300K is overpredicted by 11% by the ideal gas model, which would dwarf the Stoic engine requirement for 1% mass flow accuracy. In this paper a Helmholtz energy equation of state is employed, using the excellent open-source package CoolProp [6]. The CoolProp package is used to generate two dimensional lookup tables for property values, which are converted to a table of bicubic

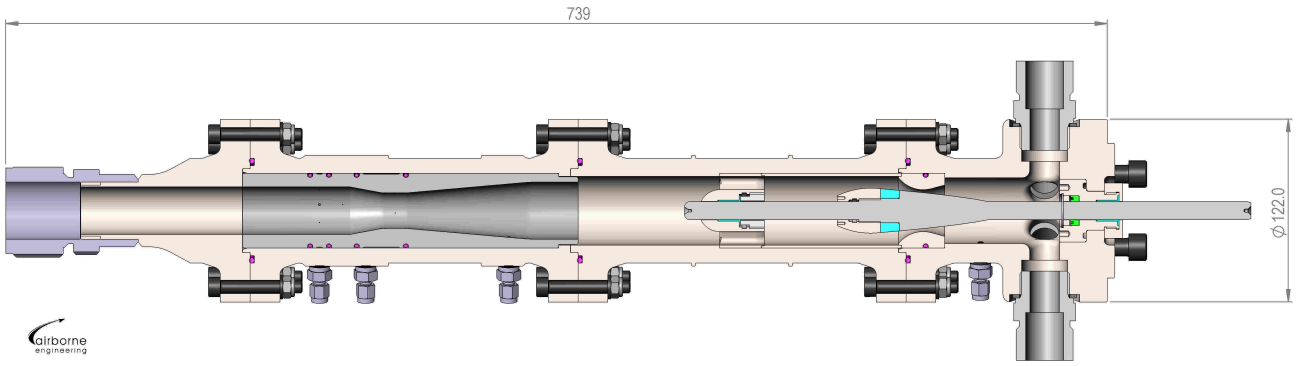

Figure 4: Cross section schematic of an automatic metering valve (AMV), showing the Venturi meter (left half) and metering valve section (right half). The linear actuator (not shown) is mounted to the pintle shaft at the right hand side of the image. All components are stainless steel apart from plastic bushings and seals (cyan) and elastomeric seals (magenta and green).

interpolation coefficients for use in the real-time calculation. Bicubic interpolation reduces the memory storage requirement on the control system microprocessor whilst maintaining lookup accuracy.

Both the full and simplified methods have been run real-time on the AMVs and the results shown to be within 1% of each other for the flow regimes tested. The simplified method was therefore used for the real-time control of the AMVs due to its lower computational overhead.

3.2.2. Metering valve

The metering valve changes the flow area by moving a tapered pintle relative to a nozzle. The pintle has a hyperbolic profile such that a change in axial distance is roughly proportional to a change in flow area. Fig. 4 shows a cross section of an AMV. The axial position of the pintle is driven by an electronic linear actuator. A KEL-F valve seat is added to the pintle such that the valve will seal completely. The valve fails in the shut position if there is a power failure.

3.2.3. Control system

The AMVs are each controlled by using an ARM Cortex M4 STM32F407 microcontroller, which runs a PID loop at 500Hz using a mass flow value that is Kalman filtered to remove noise from sensors and flow turbulence. The microcontroller then commands the position of the linear actuator to a standard servo drive. The microcontroller maintains mass flow based on either a pre-defined sequence loaded into memory, or a real-time demand via ethernet.

3.2.4. Construction

The AMVs are designed to be suitable for ground testing, rather than for flight where size and weight are very important. The AMVs are therefore designed for simplicity, ease of maintenance, ease of modification and cost. Fig. 4 shows a cross section of an AMV.

The Venturi meter has a separate casing and profiled insert, and the metering valve has a separate casing and nozzle insert. Most of the valve components are identical for all the propellants, except the inlet port, venturi insert, pintle, nozzle and outlet ports. This allows for repurposing of individual valves for different mass flows and propellants, which saves cost during the Stoic test program.

The Stoic engine requires several feed hoses for each of the propellants, so the valve outlet is manifolded to the correct number of hoses. This allows a standard linear actuator to couple to the pintle shaft at the rear of the valve, once the pintle has passed through a shaft seal. A nitrogen purge port is included downstream of the valve seal for the H_2 and O_2 lines. All components are stainless steel apart from the shaft bushings and the seals.

It is worth noting that the AMV design could be modified to suit an inline feed system, or a flight system if required. The total weight can be reduced significantly by using integral casing and nozzle profiles, by welding upstream and downstream piping directly into the valve, and by pressure balancing the pintle such that a much smaller linear actuator is required. Alternatively, a rotary metering section can be used, which has much lower weight and size and is ideal for in-line applications, but would result in higher pressure loss.

(a) *(b)*

Figure 5: Airborne Engineering's in house system for (a) manual valve control, and for (b) high-speed datalogging with simultaneous sampling. Similar data loggers are also used for thermocouples and pressure taps.

3.3. Coolant supply

The de-ionised water coolant is supplied from a tank pressurised by the main air reservoir via a dome regulator. The water is filtered before entering the engine via 14 separate hoses - required because the Stoic engine is not internally manifolded with a sufficient distribution plate or scroll. Fig. 6a shows the incoming water feed (bottom left) and water inlet and outlet hoses rising from manifolds on the floor below the engine. Four separate outlet hoses (right) discharge into a catch tank via calibrated chokes.

Pressure sensors measure the pressure drop across the discharge choke of each outlet feed, and thermocouples measure the temperature difference between the common input and the four separate outlet feeds. This allows the four coolant mass flows and heat transfers to be calculated by calorimetry.

3.4. Instrumentation

Some of the tests in the AN programme last only a second in duration and have dynamic events, such as ignition and flow transition in the nozzle. Consequently, high speed datalogging is required with simultaneous sampling across all channels - which is particularly important when correlating the nozzle flow effects with thrust side loads. All data channels are simultaneously sampled at 10kHz using AEL's in house datalogging system, which is suitable for bridge, 4-20mA and thermocouple sensors (Fig. 5b). Data is relayed via ethernet to a central Linux computer with RAID backup. A subsection of these readings is subsampled and displayed on a GUI for rig monitoring.

3.4.1. Nozzle wall pressure

The flow evolution in the altitude compensating nozzle is measured with 64 pressure taps in the nozzle wall. The pressure measurements are taken with four of AEL's in house pressure loggers, each with 16 channel detachable pneumatic fittings to make swapping nozzles easier.

3.4.2. Thrust and side loads

The thrust and side loads from the engine are measured using an AMTI MC8-10,000 6-axis load cell. The water coolant is started several seconds before ignition, so that the bellows loads from the water hoses can be removed. Bellows loads from the propellant hoses are calculated based on the pressure in the hoses and calibration coefficients. These coefficients are generated by measuring the loads when pressurising the feed systems individually with blanks at the interface between the hoses and the engine. Where geometrically possible, the feed hoses from a particular propellant are distributed evenly around the engine circumference to reduce the net side load.

3.4.3. Control and safety

The test rig is controlled by a two controllers: first, a manual valve controller (Fig. 5a) for rig isolation, filling and priming, and second, an automated valve controller for firing sequences. These sequences contain the timings for all run valves and for beginning the AMV mass flow profiles. Both valve controllers run on AEL's Touchbridge system, which allows a network of

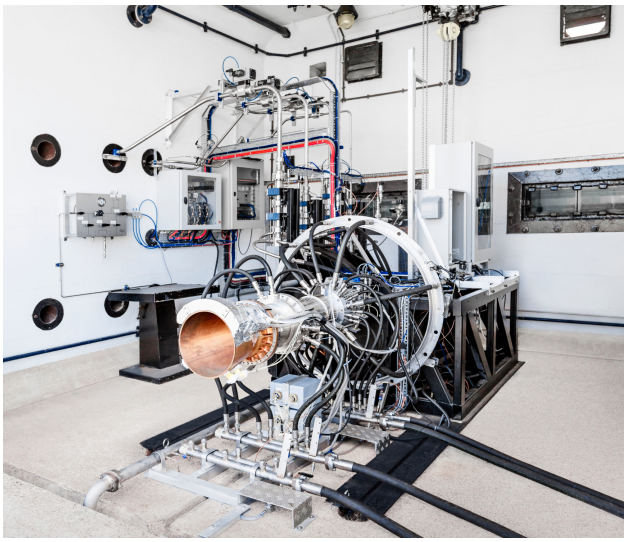

(a) Installed in J2 firing bay

(b) Firing with water-spray sound suppression

Figure 6: The Stoic engine under test at Airborne Engineering's Westcott facility.

valves, sensors or motors to be connected simply via a common 2-wire bus using a CANbus protocol. The 2-wire bus system has two main advantages: first, in reducing the quantity of wiring, and second, in removing the need for point-to-point wiring. This is useful when performing non-firing operations on the test rig; for example, when leak finding or rig commissioning, the manual valve controller (Fig. 5a) can be removed from the control room and plugged in locally where the technicians are operating.

The propellant isolator and run valves are powered through two separate 24V lines with a common off switch, which is used by the firing officer to terminate a firing sequence if required. All reservoir isolator valves are of spring-return type, and therefore both they and the AMVs fail shut if power is removed.

3.5. Automated data reduction and analysis

The Stoic test rig has over 100 data channels each sampled at 10kHz, which produces large data sets even for short firings. To improve understanding of the data, and to reduce the downtime between tests, the data is automatically analysed and summarised into a PDF file, which contains plots of all major quantities (thrust, pressures etc.) and tables of important quantities averaged in specified time windows. The software has three main stages. First, conversion of raw sensor readings into engineering units using each sensors calibration coefficients. Second, reading of the sensor data for graph plotting, averaging and calculation of relevant derived quantities (C_F, c^* etc.). Third, combination of the graphs and tables into a PDF file, with a manually entered summary of the aims of the test. Fig. 7 shows example pages from a firing report.

The automated data processing takes less than ten seconds, which together with the AMVs allows for a very efficient testing schedule; it is easy to see instantly whether a test was successful, and the AMVs then allow the firing officer to digitally specify the next engine operating condition to test. For data traceability, the rig configuration (which sensor is connected to where), the sensor calibration coefficients and the analysis software are all version controlled.

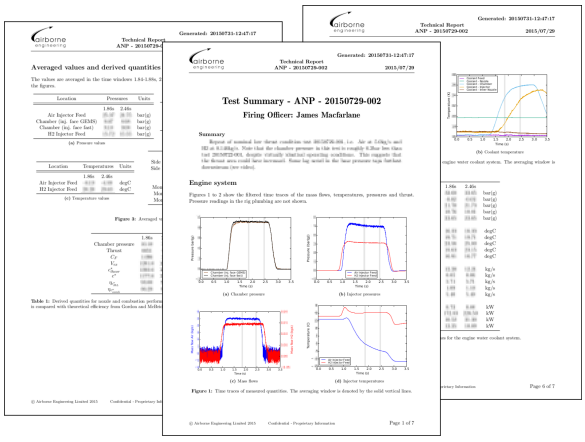

Figure 7: Example pages from an automated firing report.

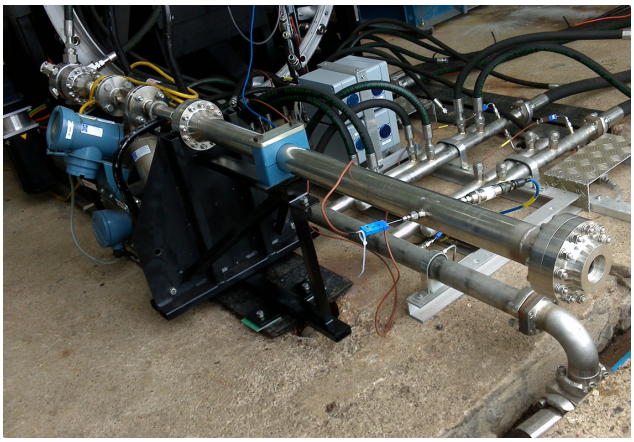

Figure 8: AMV Calibration rig with calibration tube and measured choke attached to the CMF100 coriolis meter.

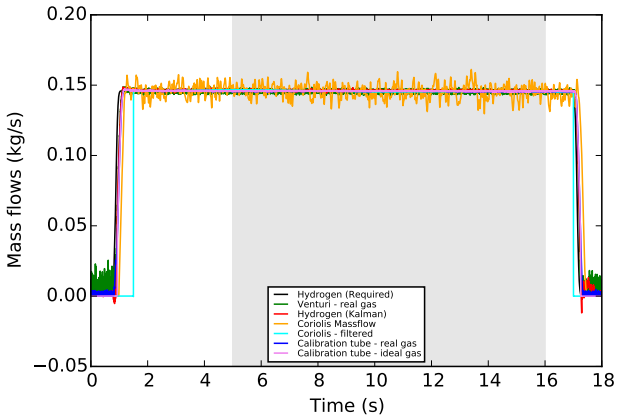

Figure 9: Mass flow profiles for a calibration run with 0.146kg/s H_2. Note the noisy coriolis meter data pre low-pass filtering. There is very good agreement between the venturi, filtered coriolis meter and calibration tube mass flow data. The gray rectangle denotes the averaging window.

4. RESULTS

The Stoic engine has been successfully fired over 30 times for a variety of operating conditions and several competing nozzle geometries. Fig. 6a shows the Stoic engine installed at the AEL Westcott J2 test facility, and Fig. 6b shows the engine firing during water-spray sound suppression experiments[1].

4.1. Mass flow regulation

To test the AMV mass flow regulation, the H_2 venturi was calibrated. Fig. 8 shows the calibration rig, where the outlet of the AMV was attached by hoses to a Micro Motion CMF-100 coriolis meter, which was in turn connected to a long settling tube which ends in a machined choke (a purely convergent nozzle). The primary purpose of the choke is to provide back pressure to keep flow velocities low in the coriolis meter, but because the settling tube ("calibration tube") contains a thermocouple and pressure sensor, the data from these sensors and the choke diameter can be used to verify the coriolis meter mass flow readings.

The CMF-100 coriolis meter is calibrated to 0.35% accuracy on mass flow, but requires a large degree of low pass filtering for gases. The manufacturer recommends that the onboard filter on the coriolis meter be set to have a time constant of >2.56s for gases. It was therefore impractical to use their onboard filtering for short step profiles of gas flow, because the gas would have to be run for at least 6 time constants (>15s) before the reading would be within 1% accuracy, and there would be a huge time lag in the results. The onboard low pass filter was therefore turned off, and low pass filtering applied to the plateaued part of data afterwards using a double pass forward-backward procedure so that no time lag was introduced.

Table 1: Time averaged mass flow data from Fig. 9.

Mass flow	kg/s
Required	0.1460
Venturi - real gas	0.1455
Venturi - Kalman filtered	0.1461
Coriolis - raw	0.1456
Coriolis - filtered	0.1456
Calibration tube - real gas	0.1458
Calibration tube - ideal gas	0.1458

The calibration process involved specifying step profiles of constant mass flow for 16s, which the AMV would follow using internal control loops that compensate for the dropping reservoir pressure. Fig. 9 shows mass flow data from a typical run, where although the reservoir pressure drops by 10% (12 bar) the mass flow is held steady at the required value of 0.146kg/s H_2. Fig. 9 also shows that the noise from the Venturi meter data is significantly less than the unfiltered Coriolis meter data that is being used as a calibration reference.

[1] It should be noted that with ED nozzle flows, care must be taken not to spray water into the plume where it may be entrained into the recirculating wake, which depending on the operating condition may exist several diameters downstream of the nozzle exit.

Table 2: Time averaged discharge coefficients and Reynolds numbers from Fig. 9.

	Cd (%)	Re
Venturi - Kalman filtered	99.67	1.33×10^6
Calibration tube - real gas	99.91	4.00×10^5

Tab. 1 shows the time averaged mass flow values, and Tab. 2 shows discharge coefficient values as per Eq. 2.

$$C_d = \frac{\dot{m}_{coriolis}}{\dot{m}_{meas}} \tag{2}$$

The calibrated results demonstrate that the AMVs correctly maintain mass flow values whilst reservoir pressures are dropping, and that the measured mass flows are within 1% of the calibration reference. Unfortunately, because the noise on the calibration reference is so large, it is not possible to quantify the accuracy beyond 1%, even though the Venturi measurement noise is much smaller.

4.2. Wall pressures

The focus of this paper is on the test rig design for the Stoic engine, but some early non-confidential results are presented here to demonstrate the capability of the system.

The nozzle wall pressure measurements are the key marker in determining whether numerical simulations of the flow in the E-D nozzle are correct. Over all tests, the comparison against numerical results has been good. The qualitative features of the flow, such as potential flow separation, have been reproduced excellently, and the quantitative location of such separations have compared well. Fig. 10 shows a sample comparison between numerical and experimental data for a case without flow separation, which shows good agreement.

4.2.1. Flow separation

By using ramped mass flow profiles for air and H_2, it is possible to increase the mass flow in the engine whilst maintaining a set O/F ratio. This can be used to sweep through a set of operating conditions where a change occurs, such as flow separation.

Fig. 11 shows some example results for flow separation during a ramped mass flow test. The smoothly ramped mass flows (Fig. 11a) maintain the O/F ratio in the engine whilst increasing total mass flow. This smoothly increases chamber pressure (Fig. 11b). The thrust (Fig. 11c) has a marked step increase, however, at around 1.6s when the flow separates from the nozzle wall. Fig. 11d shows this separation in the two wall pressure traces, which are taken in the two averaging windows shown by the gray lines in Fig. 11a-c.

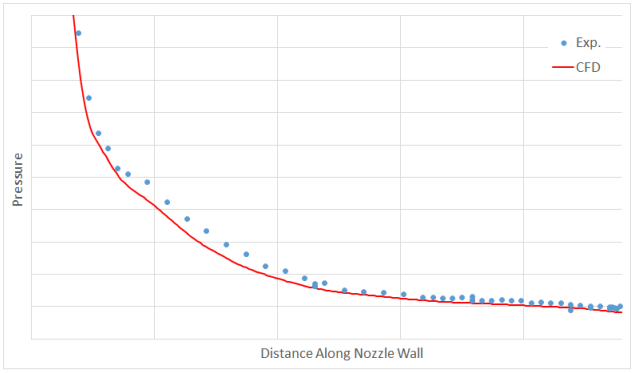

Figure 10: Stoic wall pressure readings (blue) as a function of axial distance, against numerical predictions (red), courtesy of Reaction Engines Ltd. The axes are redacted for commercial confidentiality.

5. CONCLUSIONS

The Stoic engine is successfully under test at AEL's Westcott facility, to evaluate several features of the Sabre engine at a subscale level. So far in the test programme, the numerical predictions of nozzle wall pressures have matched well with the experimental data. Qualitative features, such as flow separation, have also matched predictions well. The test programme is still underway, to evaluate the remaining outputs of the AN programme: to perform controlled transition between the air-breathing and the rocket modes, to compare the steady state heat transfer against predictive models, and to continue investigating different annular nozzle flow geometries and behaviours.

The test rig design required particular care in two areas: first, in the measurement and control of the high mass flow gaseous propellant feeds, and second, in the acquisition and dissemination of the large data sets from each test.

The Automatic Metering Valves (AMVs) designed for this project have been demonstrated to provide controlled mass flows of high pressure gaseous propellants at high flow rates (<13kg/s), with measurement accuracy of <1%. They are digitally controlled to either follow pre-defined profiles or to respond to real-time feedback of engine parameters.

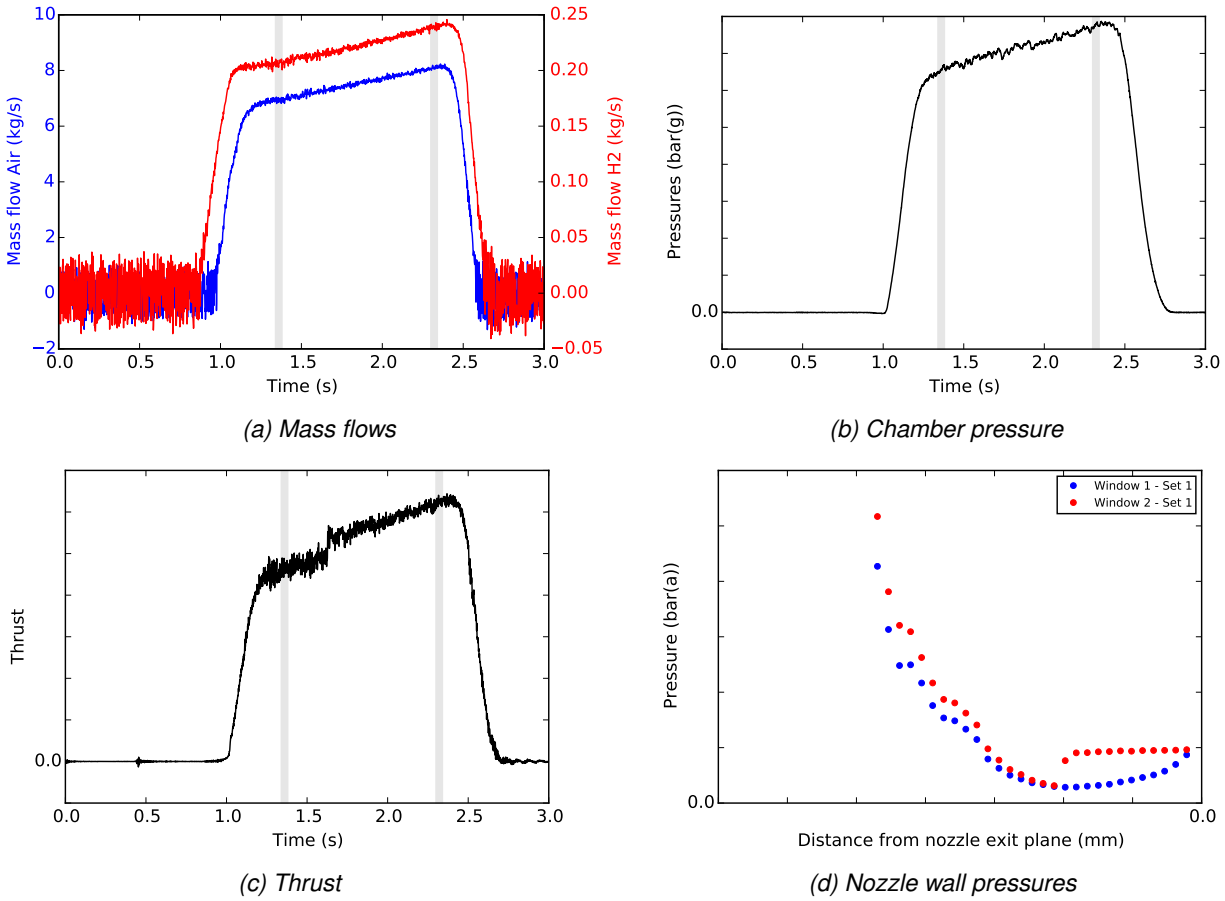

(a) Mass flows

(b) Chamber pressure

(c) Thrust

(d) Nozzle wall pressures

Figure 11: Example results for a ramped mass flow test that results in separation of the nozzle flow, courtesy of Reaction Engines Ltd. As the mass flows ramp up smoothly, the chamber pressure also ramps up smoothly, but the thrust has a noticeable step in the ramp when the flow separates. The wall pressures are shown during the two grey averaging windows.

The development of low-noise dataloggers suitable for fast data capture (10kHz), simultaneously across all channels, has allowed direct correlation between nozzle flow effects and thrust side loads. The automatic data analysis and PDF file generating software have been critical in handling the large data sets.

A particular success of the test program has been the combination of the instant test reports, the ease of valve scheduling via the Touchbridge system, and the digital control of the AMVs. This combination has allowed the firing officer to immediately know whether a test was successful, and to easily dial in the next engine operating condition, keeping the testing schedule tight and costs low.

REFERENCES

[1] Varvill, R. and Bond, A. (2004). The skylon spaceplane. *Journal of the British Interplanetary Society*, 57:22–32.

[2] Bond, A. and Webber H. (2015), Nozzle arrangement for an engine, Patent US 2015/0101337 A1.

[3] Taylor, N. V. (2011). Experimental and CFD analysis of the expansion deflection nozzle. *Proc. of 7th European Symposium of Aerothermodynamics*.

[4] Taylor N. V. et al (2011). Experimental comparison of Dual Bell and Expansion Deflection Nozzles. *47th AIAA/ASME/SAE/ASEE Joint Propulsion Conference & Exhibit*.

[5] Taylor, N. V. et al. (2010). Experimental investigation of the evacuation effect in expansion deflection nozzles. *Acta Astronautica*, 66(3-4):550–562.

[6] Bell, I. H. et al. (2014). Pure and pseudo-pure fluid thermophysical property evaluation and the open-source thermophysical property library coolprop. *Industrial & Engineering Chemistry Research*, 53(6):2498–2508.